Proc. Natl. Acad. Sci. USA
Vol. 95, pp. 6367–6372, May 1998
Medical Sciences

Angiostatin gene transfer: Inhibition of tumor growth *in vivo* by blockage of endothelial cell proliferation associated with a mitosis arrest

(angiogenesis/recombinant adenovirus/cancer)

FRANK GRISCELLI*†, HONG LI*, ANNELISE BENNACEUR-GRISCELLI‡, JEANNETTE SORIA§, PAULE OPOLON*, CLAUDINE SORIA¶‖, MICHEL PERRICAUDET*, PATRICE YEH*, AND HE LU¶

*le Centre National de la Recherche Scientifique Unite de Recherche Associée 1301/Rhône-Poulenc Rorer Gencell, Institut Gustave Roussy, 94805 Villejuif, France; ‡Service d'hématologie biologique, Institut Gustave Roussy, 94805 Villejuif, France; §Laboratoire de biochimie Aet Sainte Marie, Hôtel Dieu, 75004 Paris, France; ¶l'Institut National de la Santé et de la Recherche Médicale U353, Hôpital St. Louis, Avenue Claude Vellefaux, 75010 Paris, France; and ‖DIFEMA, faculté de Médecine, 76000 Rouen, France

Communicated by N. M. Le Douarin, College de France, Nogent-sur-Marne, France, March 16, 1998 (received for review October 24, 1997)

ABSTRACT **The antitumoral effects that follow the local delivery of the N-terminal fragment of human plasminogen (angiostatin K3) have been studied in two xenograft murine models. Angiostatin delivery was achieved by a defective adenovirus expressing a secretable angiostatin K3 molecule from the cytomegalovirus promoter (AdK3). In *in vitro* studies, AdK3 selectively inhibited endothelial cell proliferation and disrupted the G_2/M transition induced by M-phase-promoting factors. AdK3-infected endothelial cells showed a marked mitosis arrest that correlated with the down-regulation of the M-phase phosphoproteins. A single intratumoral injection of AdK3 into preestablished rat C6 glioma or human MDA-MB-231 breast carcinoma grown in athymic mice was followed by a significant arrest of tumor growth, which was associated with a suppression of neovascularization within and at the vicinity of the tumors. AdK3 therapy also induced a 10-fold increase in apoptotic tumor cells as compared with a control adenovirus. Furthermore, we showed that systemic injection of AdK3 delayed C6 tumor establishment and growth, confirming that angiostatin can function in a paracrin manner. Our data support the concept that targeted antiangiogenesis, using adenovirus-mediated gene transfer, represents a promising alternative strategy for delivering antiangiogenic factors as their bolus injections present unsolved pharmacological problems.**

The formation of blood vessels, or angiogenesis, results from the capillary growth of preexisting vessels. Angiogenesis is essential for a number of physiological processes such as embryonic development, wound healing, and tissue or organ regeneration. Abnormal growth of new blood vessels occurs in pathological conditions such as diabetic retinopathy and tumor growth, as well as tumor dissemination to distant sites (1, 2). Experimental and clinical studies have showed that primary tumors as well as metastases can remain dormant because of a balanced rate of proliferation and apoptosis unless the angiogenesis process is switched on (3). The growth of endothelial cells is tightly regulated by both positive and negative factors. The onset of tumor angiogenesis could be triggered either by an up-regulation of tumor-released angiogenic factors such as vascular endothelial growth factor and acid and/or basic fibroblast growth factor or by a down-regulation of angiostatic factors such as thrombospondin and angiostatin (3). The reconstitution of angiostatic factors and/or the removal of angiogenic stimulating factors thus constitute plausible clinical strategies to suppress tumor angiogenesis (4–9). Angiostatic-based therapies should also apply to all solid tumors because endothelial cells do not vary from one tumor type to the other, further emphasizing the clinical relevance of such an anticancer approach.

Many physiological angiostatic factors are derived upon proteolytic cleavage of native proteins. This is the case for angiostatin (6), endostatin (7), the 16-kDa fragment of prolactin (8), or platelet factor-4 (9). Angiostatin was initially isolated from mice bearing a Lewis lung carcinoma, and was identified as a 38-kDa internal fragment of plasminogen (Plg) (amino acids 98–440) that encompasses the first four kringles of the molecule (6). Angiostatin has been shown to be generated following hydrolysis of Plg by a metalloelastase from granulocyte–macrophage colony-stimulating factor-stimulated tumor-infiltrating macrophages (10). S.c. bolus injections of purified angiostatin in six different tumor models have proved to be very effective in suppressing primary tumor growth, with no apparent toxicity (11). Angiostatin-mediated suppression of tumor angiogenesis apparently drove the tumor cells into a higher apoptotic rate that counterbalanced their proliferation rate. In this study, tumor growth usually resumed following removal of the angiostatin molecule, emphasizing the importance of achieving long-term delivery for optimal clinical benefits (11). *In vitro* studies with recombinant proteins indicated that the angiostatic activity of angiostatin was mediated mostly by kringles 1–3, with a minor activity for kringle 4 (12). As for most angiostatic factors, little is known about the molecular pathway by which angiostatin exerts its effect.

Because angiostatic therapy will require a prolonged maintenance of therapeutic levels *in vivo*, the continuous delivery of a recombinant protein will be expensive and cumbersome. Direct *in vivo* delivery of the corresponding genes with viral vectors constitutes an attractive solution to this problem. Because most cancer gene therapies currently rely on destructive strategies that target the tumor cells (13), viral-mediated gene delivery of an angiostatic factor represents a conceptually different, and possibly synergistic, approach to fight cancer. In this study, we constructed a defective adenovirus that expresses the N-terminal fragment (amino acids 1–333) from human Plg, including the preactivation peptide and kringles 1

The publication costs of this article were defrayed in part by page charge payment. This article must therefore be hereby marked "*advertisement*" in accordance with 18 U.S.C. §1734 solely to indicate this fact.

Abbreviations: CMV, cytomegalovirus; Plg, plasminogen; pfu, plaque-forming units; moi, multiplicity of infection; HMEC, human microcapillary endothelial cells; vWF, von Willebrand factor; Ad, adenovirus.

A commentary on this article begins on page 5843.

†To whom reprint requests should be addressed. e-mail: grisceli@igr.fr.

to 3, and we assessed its *in vitro* and *in vivo* activity in different murine tumor models.

MATERIALS AND METHODS

Construction of AdK3. AdK3 is an E1-defective recombinant adenovirus that expresses the N-terminal fragment of human plasminogen (up to residue 333) from the cytomegalovirus (CMV) promoter. Plasmid PG5NM119 containing the human Plg cDNA was provided by J. Castellino (University of Notre Dame, IN). A fragment encoding the 18 aa signal peptide of Plg, followed by the first 326 residues of mature Plg was first subcloned between the *Bam*HI and *Sca*I sites of plasmid pXL2675. A synthetic oligodeoxynucleotide encoding residues 327–333 followed by a stop codon was then added, before inclusion between the CMV promoter and the SV40 late polyadenylation signal. This expression cassette was then inserted between the *Eco*RV and *Bam*HI sites of plasmid pCO5 to generate plasmid pCO5-K3. AdK3 was constructed in 293 cells by homologous recombination between pCO5-K3 and *Cla*I-restricted adenovirus DNA extracted from an adenovirus carrying the β-galactosidase gene driven by the Rous Sarcoma virus promoter (AdRSVβgal) (14). Individual plaques were isolated onto 293-derived cell monolayers and amplified onto fresh 293 cells, and viral stocks were prepared as described (14). AdCO1 is a control virus that is identical to AdK3 except that it does not carry any expression cassette.

Cell Lines Maintenance and Infection. C6 glioma cells [American Type Culture Collection (ATCC) CCL-107] and MDA-MB 231 cells (ATCC HTB 26) were cultured in DMEM with 10% of fetal calf serum. Viral infection was performed with 5% fetal calf serum. Human microcapillary endothelial cells (HMEC-1) (15) were cultured in MCDB 131 (GIBCO/BRL) supplemented with 20% of fetal calf serum, 1 mM L-glutamine, 1 μg/ml hydrocortison, and 10 ng/ml epithelium growth factor, and infection was performed in the same medium but with 10% of fetal calf serum and 3 ng/ml recombinant human basic fibroblast growth factor (R & D Systems). The multiplicity of infection (moi) was chosen as to obtain between 80% and 100% infected cells as judged by 5-bromo-4-chloro-3-indolyl β-D-galactoside staining after infection with virus AdRSVβGal (14).

Western Blot Analysis. Subconfluent cells were infected with AdK3 or AdCO1 at an moi of 300 plaque-forming units (pfu)/cell. Cell culture supernatants were collected 48–96 hr postinfection (p.i.). For *in vivo* immunological analysis of the K3 angiostatin molecule, the tumors were collected at day 10 p.i., frozen in liquid nitrogen, powdered, extracted with lysis buffer (10 mM *N*-ethylmaleimide/1% Triton X-100/1 mM phenylmethylsulfonyl fluoride/0.1M NH_4OH) and centrifuged at 12,000 rpm at 4°C. The samples with 300 μg of protein were run in a 10% SDS-polyacrylamide gel before being transferred onto a nitrocellulose membrane (Schleicher & Schuell). As a control, 100 ng of human Plg (Stago, Asnieres, France) was run. After a 2-hr incubation in blocking buffer (TBS-5% milk–0.05% Tween 20), the membranes were incubated for 1 hr with anti-human Plg MAb A1D12 (16) and 1 hr with a horseradish peroxidase-conjugated goat anti-mouse serum (Biosys, Compiegne, France). After washing, the membranes were revealed with enhanced chemiluminescence–bioluminescence kit (Amersham). To detect the phosphorylated epitope of mitotic-specific proteins, the extracts were prepared from the HMEC-1 cell 96 hr p.i. and probed with a specific mAb (clone MPM-2 from DAKO).

Proliferation Assay. Tumor or HMEC-1 cells were infected with AdK3 or AdCO1 at the indicated moi for 12 hr. The cells were collected with 1 mM EDTA, washed twice with PBS, and resuspended. They were seeded into 96-well culture plates (5,000 cells/well) and cultured for 72 hr. In addition, HMEC-1 cells were cultured in MCDB131 medium containing 40, 20, or 10% supernatant of AdK3 or AdCO1-transduced C6 glioma cells. Supernatants from virally infected C6 cells were collected 96 hr p.i., heated 30 min at 56°C to inactivate the virus, concentrated 10 times, and dialyzed against PBS. Cells were quantified with a cell proliferation assay kit by using a 4,5 dimethylthiazol-3-carboxymethoxy-phenyl-4-sulfophenyl-tetrazolium (MTS) tetrazolium compound (Promega).

Formation of Capillary Tube in a Fibrin Matrix Model. This model was devised according to the method of Pepper *et al.* (17) using calf pulmonary artery endothelial cells (CPAE; ATCC, CCL 209) infected for 12 hr with AdK3 or AdCO1 at an moi of 600.

Whole Blood Lysis Assay. Whole blood clot lysis was performed by mixing 80 units/ml of tissue-plasminogen activator, 250 μl of culture supernatant obtained 4 days p.i. with AdK3 or AdCO1, and 500 μl of citrate-anti-coagulated whole blood collected from healthy donors. Coagulation was triggered by adding 1 unit/ml of thrombin and 12 mM Ca^{2+}. The extent of clot lysis was determined by lysis time and by following the kinetics of soluble D-Dimers as described (18).

Immuno Flow Cytometry. HMEC-1 were infected for 96 hr with AdK3 or AdCO1 at an moi of 300 pfu/cell. The cells were collected, permeabilized with Triton X-100, and incubated with propidium iodide (20 μg/ml) and ribonuclease A (100 μg/ml) for 30 min at room temperature to label DNA before incubation with mitotic MPM-2 antibody as described (19). Fluorescein isothiocyanate-conjugated anti-mouse IgG antibodies were used to detect MPM-2 phosphoepitope. The experiment was performed in a Coulter EPICS Profile II flow cytometer, and the data were analyzed by MULTICYCLE software (Phoenix Flow Systems, San Diego, CA).

Athymic Murine Models. Cultured C6 glioma cells and MDA-MB-231 cells were harvested, washed, and resuspended in PBS at 1.5×10^7 and 0.25×10^7cells/ml respectively, and a volume of 200 μl was injected s.c. into the dorsa of 6- to 7-week-old nude mice. When the tumors had reached a volume of 20 mm^3, the animals received an intratumoral injection of 10^9 pfu of either AdK3 ($n = 6$), AdCO1 ($n = 6$), or PBS ($n = 6$). Tumor size was monitored until day 10 p.i. for the C6 glioma model and day 42 p.i. for the MDA-MB-231 model.

To assess the effect of AdK3 infection on tumor establishment and progression, C6 cells were infected *in vitro* for 24 hr with AdK3 or AdCO1 at an moi of 100 pfu/cell before s.c. inoculation. A PBS suspension of 200 μl containing 5×10^5-infected C6 cells was injected into the dorsa of nude mice ($n = 6$). To prove that angiostatin has a dose-dependent effect, AdK3 or AdCO1-infected C6 glioma cells were mixed at a ratio of 1:2 and 1:4 with noninfected C6 cells to a total of 5×10^5 cells, before implantation. In another experiment, MDA-MB-231 cells were infected at an moi of 50 pfu/cell. Infected MDA-MB-231 cells are less tumorigenic than infected C6 cells so 80 μl of ice-cold Matrigel (Becton Dickinson) had to be added to 120 μl of PBS containing 10^6 MDA-MB-231-infected cells before s.c. implantation. Tumor establishment and growth were followed until day 25 (MDA-MB-231) or day 20 (C6) p.i.

To test whether angiostatin can function in a paracrin manner 5×10^9 pfu of AdK3 or AdCO1 was injected i.v. into the retroorbital vein of nude mice ($n = 5$), 24 hr before s.c. implantation of 2.5×10^5 C6 cells. Tumor establishment and growth were followed until day 20 p.i. A Student's *t* test was performed for statistical analysis.

Immunohistochemistry. Tumor tissues were fixed in alcohol formalin acetic acid and embedded in paraffin, and 5-μm sections were prepared. After toluene treatment and rehydratation, the sections were pretreated three times for 5 min in a microwave oven in 10 mM citrate buffer (pH 6.0), quenched by 3% H_2O_2 for 5 min to remove endogenous peroxidase activity, washed in PBS, and then incubated with a rabbit polyclonal serum raised against human von Willebrand

factor (vWF; Dako, dilution 1:200) for 60 min. After three washes, the sections were incubated with biotinylated goat anti-rabbit IgG antibodies for 30 min, washed, and incubated with streptavidin-peroxidase for 30 min before addition of 3-Amino-9-ethyl-carbazole. Meyer's hematoxylin was used for counterstaining. Apoptotic cells within the section were detected by a kit using a terminal deoxynucleotidyltransferase-mediated dUTP-biotin nick end labeling method (TUNEL; Boehringer Mannheim). For proliferating cell nuclear antigen staining procedure included a biotinylated mouse anti-proliferating cell nuclear antigen antibody (PharMingen, dilution 1:100) followed by streptavidin peroxidase and substrate revelation.

RESULTS

Molecular Characterization of AdK3. Recombinant AdK3 carries a CMV-driven N-terminal fragment of human Plg that includes the first three kringle domains of the angiostatin molecule (12), whereas AdCO1 is an "isogenic" control adenovirus that does not encode any expression cassette (Fig. 1*A*). Secretion of the K3 molecule in the culture media 2–3 days after infection with AdK3 was demonstrated for HMEC-1, C6, and MDA-MB-231 cells by mAb A1D12 immunoblotting, whereas no signal was detected following infection with AdCO1 (Fig. 1*B*). The secreted immunoreactive peptide appeared as a doublet with a molecular mass of 36 and 38 kDa, most likely reflecting a different extent of *N*-glycosylation at Asn^{289} as described for Plg (20, 21).

Functional Characterization of AdK3. Transduction of HMEC-1 by AdK3 resulted in an inhibition of basic fibroblast growth factor-stimulated proliferation in a dose-dependent manner at day 3 p.i.: 30% at an moi of 50, 74% at an moi of 150, and 97% at an moi of 300, in sharp contrast to the cells infected with AdCO1 ($P < 0.005$). AdK3 did not affect MDA-MB-231 and C6 cell proliferation (Fig. 2*A*). To assess the paracrine potential of the K3 molecule to exert these effects, virus-free culture media from virally infected C6 glioma cells were added to HMEC-1 cells. As illustrated in Fig. 2*A*, we did observe a dose-dependent inhibition of HMEC-1 cell proliferation by C6 cell-secreted angiostatin ($P < 0.001$). The addition AdK3 also significantly inhibited the capillary formation of CPAE cells in fibrin gel with a 55% mean reduction (not shown). Moreover, whole blood clot lysis induced by tissue type plasminogen activator was not inhibited by the addition of cell culture supernatants from AdK3-infected C6 cells, and the generation of D-Dimers was basically unchanged during the first 3 hr (1,200 ng/ml vs. 1,150 ng/ml).

AdK3 Inhibits Mitosis of Endothelial Cells. To determine whether angiostatin is able to block the mitosis of HMEC-1, a flow immunocytometry analysis was performed with the cells labeled with mAb MPM-2 that binds to the phosphrylated

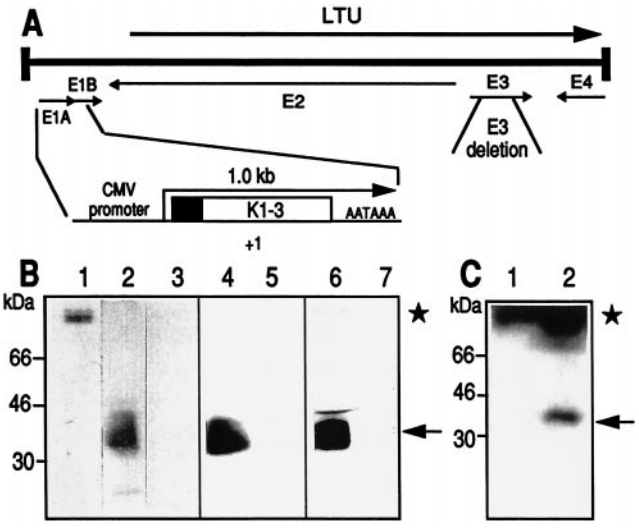

FIG. 1. Recombinant adenoviruses. (*A*) The Ad5 genome is a 36-kilobase long chromosome. Viruses AdK3 and AdCO1 were derived by a lethal deletion of the E1 genes (nucleotides 382 to 3446); they also carry a nonlethal 1.9-kilobase *Xba*I deletion within region E3 (for a review, see ref. 23). The angiostatin expression cassette is shown under the Ad5 chromosome. The plasminogen secretion signal is represented by a blackened box; +1 refers to the CMV-driven transcription start; AATAAA refers to the SV40 late polyadenylation signal. (*B*) Analysis of angiostatin secretion from infected cells. One hundred nanograms of human Plg (lane 1), culture medium from HMEC-1 infected with AdK3 (lane 2) or AdCO1 (lane 3), C6 infected with AdK3 (lane 4) or AdCO1 (lane 5), and MDA-MB-231 infected with AdK3 (lane 6) or AdCO1 (lane 7) were submitted to Western blot analysis. (*C*) Immunodetection of angiostatin within C6 tumor extracts; Tumors were established in nude mice and received 10^9 pfu of AdCO1 (lane 1) or AdK3 (lane 2), and Western blot analysis was performed 10 days p.i. The signal corresponding to angiostatin (36–38 kDa) and Plg (92 kDa) are indicated (arrow and asterisk, respectively).

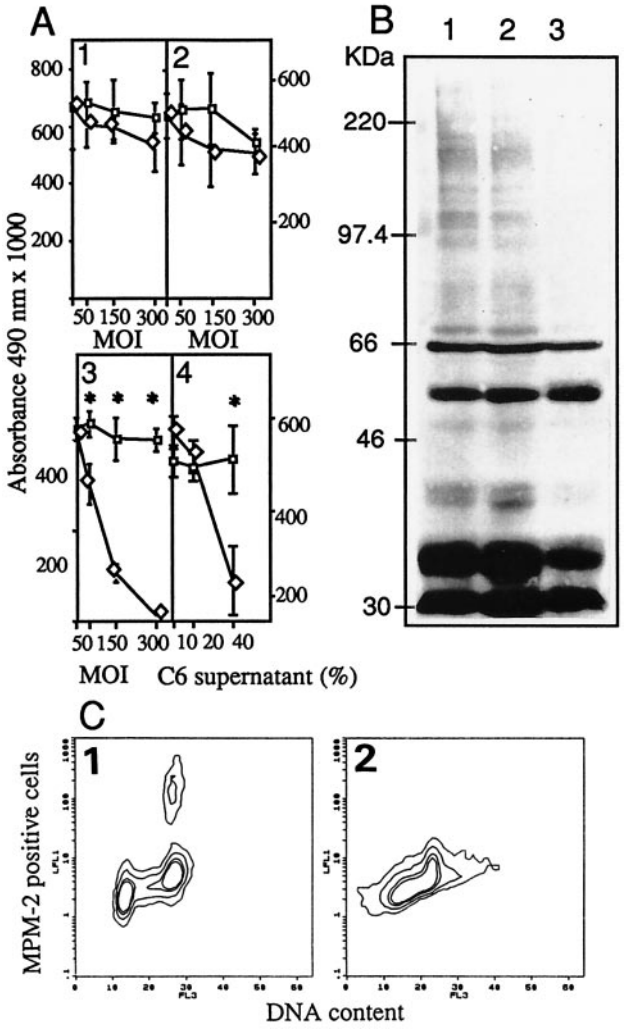

FIG. 2. (*A*) Inhibition of endothelial cell proliferation. C6 (*1*), MDA-MB-231 (*2*), and HMEC-1 (*3*) were injected with AdK3 (◇) or Ad-CO1 (□). HMEC-1 cells (*4*) cultured with the supernatant from AdK3- (◇) or AdCO1-infected C6 glioma cells (□). (*B*) Detection of MPM-2 phosphoepitope in HMEC-1 cells. Mock-infected cells (*1*), AdCO1-infected cells (*2*), and AdK3-infected cells (*3*). (*C*) MPM-2 epitope were detected in HMEC-1 infected with AdCO1 (*1*) or AdK3 (*2*) by indirect immunostaining and DNA content by propidium iodide staining, and quantified by flow cytometry (see *Materials and Methods*). A Student's *t* test was used for statistical analysis.

proteins specifically present during the M-phase, together with concurrent DNA staining. The results showed that mitosis of AdK3-infected HMEC-1 cells was decreased by 82% relative to AdCO1 infection: only 5% of HMEC-1 cells within the G_2/M peak scored positive for MPM-2 following infection with AdK3 as compared with 27% following AdCO1 control infection (Fig. 2*C*). Western blot analysis was performed from HMEC-1 extracts to detect MPM-2 positive proteins as at least 16 mitotic phosphoproteins were usually revealed by MPM-2 with an apparent molecular mass ranging from 40 to >200 kDa. As compared with control extracts from noninfected or AdCO1-infected HMEC-1 cells, extracts from AdK3-infected cells exhibited a markedly reduced level of MPM2-reactive phosphoproteins (Fig. 2*B*).

AdK3 Inhibits Tumor Growth. To induce local secretion of angiostatin, a single dose of 10^9 pfu of AdK3 was injected into 20 mm^3-preestablised human MDA-MB-231 breast carcinoma and rat C6 glioma tumors grown in athymic mice, and tumor growth was monitored. As shown in Fig. 3*A*, C6 tumors from the AdK3-injected group were significantly smaller than those from the AdCO1 or the PBS control groups: at day 10 p.i., AdK3-injected tumors had reached a mean volume of 278 ± 14 mm^3 vs. 1403 ± 142 mm^3 or 1583 ± 259 mm^3 for AdCO1- and PBS-injected tumors, respectively ($P < 0.05$). This 80% inhibition correlated with the detection of angiostatin-immunoreactive material (Fig. 1*C*). As shown in Fig. 3*B*, tumor growth was similarly inhibited (85%) in the MDA-MB-231 tumor model at day 42 p.i.: 80 ± 4 mm^3 for AdK3-treated tumors vs. 563 ± 137 mm^3 for AdCO1- and 530 ± 69 mm^3 for PBS-injected tumors respectively ($P < 0.05$).

AdK3 Inhibits Angiogenesis and Induces Tumor Cell Apoptosis *in vivo*. C6 tumors injected with AdCO1 appeared much more vascularized than their AdK3-infected counterparts (Fig. 4 *A* and *B*). Intratumoral angiogenesis was thus assessed by vWF-immunostaining of tumor sections as described (22). vWF-positive hotspots were localized first at low magnification, and vWF-positive vessels were then counted at 200X magnification (Fig. 4 *E* and *F*). The results indicated a marked reduction of intratumoral vascularization within AdK3-injected tumors (5 ± 2 vWF-positive vessels/field) as compared with the AdCO1-injected control (14 ± 4; $n = 5$, $P < 0.005$). Tumors in the PBS-injected group exhibited an identical number of vessels (14 ± 3), indicating that the infection conditions used did not interfere with tumor angiogenesis. At the macroscopic level, C6 tumors injected with AdK3 displayed little peripheral neovascularization as compared with

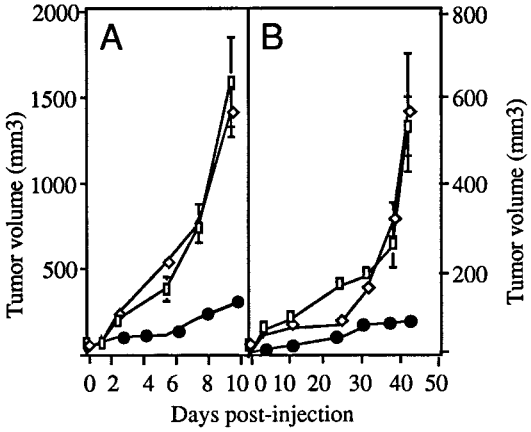

FIG. 3. AdK3 inhibits tumor growth. C6 glioma (*A*) and MDA-MB-231 carcinoma (*B*) were s.c. implanted into athymic mice (see *Materials and Methods*). When the tumor had reached a volume of 20 mm^3 (day 0), mice received an intratumoral injection of PBS (□), 10^9 pfu of AdK3 (●), or AdCO1 (◇). Mean values are represented with their standard deviations.

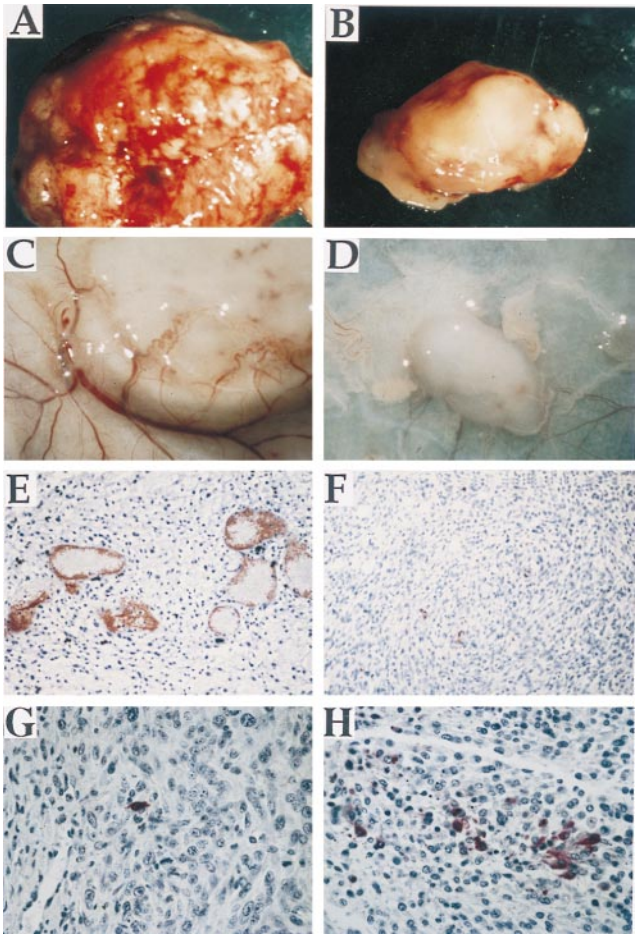

FIG. 4. AdK3 inhibits C6 tumor growth and angiogenesis. Tumors from AdCO1-treated (*A*) and AdK3-treated groups (*B*) are shown 10 days p.i. The extent of vascularization at the periphery of a representative tumor injected with AdCO1 (*C*) or AdK3 (*D*) is shown at day 5 p.i. Paraffin-embeded C6 sections from an AdCO1-injected (*E*) or AdK3-injected tumor (*F*) were submitted to vWF-immunostaining at day 10 p.i. The proportion of apoptotic cells was detected by the TUNEL method within sections from an AdCO1-injected (*G*) or AdK3-injected tumor (*H*). The same magnification was used for AdCO1- and AdK3-injected tumors.

their AdCO1-treated counterparts (Fig. 4 *C* and *D*). Similar results were obtained within MDA-MB-231 tumor sections (4.8 ± 1.2 vWF-immunoreactive vessels/field for AdK3 vs. 15.6 ± 3 for AdCO1, $P = 0.02$). Tumor cell apoptosis was then quantified *in situ* with the C6 tumor samples by the TUNEL method (see *Materials and Methods*). The results indicated a marked increase of apoptotic cells in the AdK3-injected C6 tumors 10 days p.i. (20 ± 9 vs. 1–2 apoptotic cells/field for control tumors, $P < 0.001$) (Fig. 4 *G* and *H*). In contrast, the tumor cell proliferation rate was not different among the three animal groups as assessed by proliferating cell nuclear antigen immunostaining (not shown).

AdK3 Inhibits Tumorigenesis and Tumor Growth. To question whether inhibition of tumor angiogenesis attenuated tumorigenesis, C6 and MDA-MB-231 cells were first infected for 24 hr before injection into the dorsa of nude mice. After 9 days, all of the mice from the AdCO1-infected group developed hypervascularized C6 tumors with an average size of 50 ± 7 mm^3, whereas 66% of animals from the AdK3-infected group remained tumor free. The remaining animals exhibited very small tumors (average size of 4.4 ± 1.5 mm^3) that were hardly vascularized. After 20 days, the tumors that were observed within the AdK3 group were at least 7-fold smaller than those from the AdCO1 group ($n = 6$, $P < 0.05$). Similar observations

were made with the MDA-MB-231 tumor model (not shown). C6 cells were then mixed with different ratios (1:2 and 1:4) with noninfected C6 cells before implantation to confirm the efficiency of the secreted angiostatin. As illustrated in Fig. 5, after 20 days, a dose-dependent effect of the secreted angiostatin was observed when varying the ratios of infected vs. noninfected C6 cells. Furthermore, the control group evidenced the noncytotoxicity of the control recombinant adenovirus, underlining in this manner the tumor growth inhibition effect of the angiostatin peptide.

Systemic Injection of AdK3 Prevents C6 Glioma Establishment and Tumor Growth. To question whether secreted angiostatin can function in a paracrin manner, high doses of AdK3 and AdCO1 were injected i.v. to infect a wide range of tissues able to secrete angiostatin, 24 hr before C6 glioma tumor establishment. Nine days after C6 cells implantation, all of the mice from the AdCO1-treated group developed tumors, whereas 80% of animals from the AdK3-treated group remained tumor free. After 20 days, the tumors size within the AdK3 group were 70% smaller than those from the AdCO1 group (158 ± 30 vs. 567 ± 66, $P < 0.05$).

DISCUSSION

Angiostatin has been shown to be a physiopathological inhibitor of angiogenesis secreted by primary tumors, driving the metastasis into a dormant state. However, s.c and i.p. bolus injections of human angiostatin have underlined difficult pharmacological problems because angiostatin is rapidly cleared from the circulation (11, 6). A prolonged exposure of purified angiostatin at high doses was indeed required to maintain cytostatic intratumoral concentrations of angiostatin (11). Direct transduction of the tumor and the surrounding tissue with a recombinant virus encoding an angiostatin cDNA may thus represent a more efficient method of achieving constant long-lasting intratumoral concentrations of angiostatin. Adenoviruses are appropriate vectors in such a strategy as they can efficiently express their transgene at therapeutic levels in both proliferating and nonproliferating cells (for a review, see ref. 23), allowing to target a wide area for angiostatin production. We thus have constructed a defective adenovirus that expresses the N-terminal fragment (amino acids 1–333) from human Plg, including its preactivation peptide and kringles 1 to 3 (AdK3). The use of mAb A1D12, which is specific to human Plg (16), first demonstrated an efficient secretion of angiostatin in the culture media of cells infected with AdK3.

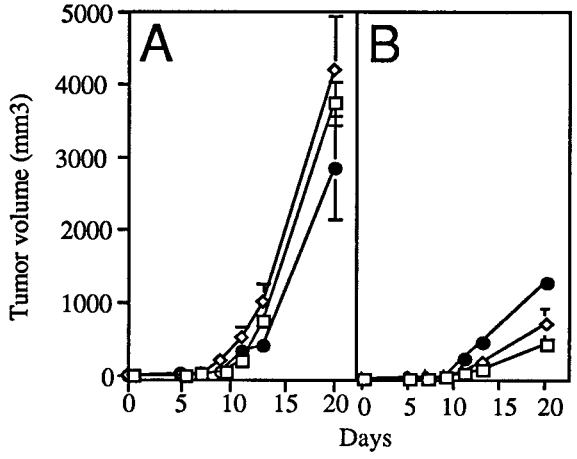

FIG. 5. Dose-dependent effect of AdK3. C6 cells were infected *in vitro*, 24 hr with AdCO1 (*A*) or AdK3 (*B*), and mixed at a ratio of 1 (□), 1:2 (◇), and 1:4 (●) with noninfected C6 cells before implantation into athymic mice ($n = 6$). Tumor volumes were measured during 20 days. Mean values are represented with their standard deviations.

The inclusion of the N-terminal preactivation peptide in the angiostatin molecule did not affect its anti-angiogenic activity because AdK3-, but not AdCO1-infected endothelial cells, showed a marked, dose-dependent arrest in proliferation *in vitro* (Fig. 2*A*). Furthermore, the proliferation of MDA-MB-231 or C6 tumor cells was not affected by AdK3-infection, demonstrating the restricted action of angiostatin for endothelial cells. Virus-free supernatants from AdK3-infected tumor cell culture also inhibited endothelial cells proliferation, illustrating the paracrine effect of angiostatin secreted by transduced tumor cells. Because the kringle domains are important for Plg binding to fibrin and fibrin degradation, it was essential to analyze the effect of this therapy in thrombolysis, a physiological protection against thrombosis *in vivo*. We showed that the angiostatin secreted in the culture medium failed to inhibit tissue type plasmingen activator-induced whole blood clot lysis *in vitro*. Although this experiment has not excluded the deleterious competition between angiostatin and Plg to bind to fibrin during thrombolysis *in vivo*, it did indicate that angiostatic effect could be achieved at a concentration far below than that required for abrogating plasminogen-dependent thrombolysis *in vivo*. This result also may suggest that endothelial cells exhibit a receptor which recognizes angiostatin and not intact Plg.

Flow cytometry analysis of endothelial cells infected with AdK3 demonstrated a complete disappearance of the mitotic population positive for MPM-2 mAb (24). Immunoblot revealed that M-phase phosphoproteins reactive to MPM-2 mAb were indeed down-regulated in angiostatin-treated endothelial cells, in sharp contrast with control endothelial cells. This observation should be helpful to define the mechanism by which angiostatin abrogates the proliferation of endothelial cells. We also showed that angiostatin disrupted the G_2/M transition induced by M-phase-promoting factor, composed of cdc2 and its associated regulatory subunit, cyclin B (25). M-phase-promoting factor-phosphorylated proteins, reactive with MPM-2 mAb, are involved in major alterations of cellular structures and activities for an efficient progression to mitosis. The reason why active M-phase-promoting factor was lacking in AdK3-transduced endothelial cells must be further investigated.

A single intratumoral injection of AdK3, but not of AdCO1, was shown to dramatically inhibit primary tumor growth in two preestablished xenograft murine models. This inhibitory effect on tumor growth was tightly correlated with a markedly decreased vascularization within, and at the vicinity of the tumors (Fig. 4), together with the detection of angiostatin-immunoreactive material in the tumor extracts (Fig. 1*C*). C6 glioma is a highly vascularized tumor due to its vascular endothelial growth factor overexpression (26). Interestingly, the AdK3-transduced C6 glioma apparently failed to establish a vascular network within the tumor mass to support rapid and extensive growth (Fig. 4), and this failure translated to >80% inhibition of tumor growth. vWF immunostaining of tumor sections also revealed a significant reduction of neoangiogenesis in the AdK3-treated tumors: well formed vessels with a mature lumen were observed frequently in control C6 tumors but not in AdK3-treated C6 glioma (Fig. 4). This decrease in vessel density was associated with a 10-fold increase in tumor cells apoptosis and no apparent modification of the tumor cell proliferation index, probably because: (*i*) of the lack of endothelial-derived paracrine factors, (*ii*) a reduction in nutriment support, and (*iii*) hypoxy-triggered p53-dependent apoptosis of the tumor cells (27, 28). In the MDA-MB-231 breast carcinoma model, a single intratumoral injection of AdK3 similarly induced a remarkable inhibition of tumor angiogenesis and growth.

In the course of this study, we also noticed that AdK3-transduced C6 and MDA-MB-231 cells exhibited a lower tumorigenic potential as reflected by a prolonged delay for

AdK3-infected cells to develop into visible tumors following implantation. Furthermore, tumor growth inhibition proved to be AdK3 dose-dependent (Fig. 5). We also showed that systemic injection of AdK3 delayed C6 tumor establishment and growth, which highly confirmed the paracrin activity of the secreted angiostatin.

Angiostatic therapy using recombinant adenoviruses has been shown to be experimentally plausible and efficient. Nevertheless, that AdK3 failed to completely abolish tumorigenesis underlines the importance of improving the vectorization of the angiostatic cDNA so that a sustained expression can be achieved for maximum clinical benefits. The possibility of delivering more than one angiostatic factor also could synergize to arrest tumor growth. It also is envisioned that its association with cytotoxic approaches may be particularly potent to improve the clinical outcome of malignant diseases.

We thank E. Faure and P. Ardouin (Intitut Gustave Roussy, Villejuif) for animal care, A. Verwish for flow cytometry measurements, E. Connault for technical assistance, and Ades & Lawley for providing the HMEC-1 cell line. We also acknowledge K. A. Larsen for helpful advice and interest and M. Mackenthun for critical reading. We thank Prof. J. Castellino for providing us with the PG5NM119 plasmid containing human pfg cDNA. La Ligue Nationale Contre Le Cancer, le Centre National de la Recherche Scientifique (CNRS), and l'Institut National de la Santé et de la Recherche Médicale (INSERM) are acknowledged for financial support.

1. Folkman, J. (1990) *J. Natl. Cancer Inst.* **82,** 4–6.
2. Folkman, J. (1995) *Nat. Med.* **1,** 27–31.
3. Hanahan, D. & Folkman, J. (1996) *Cell* **86,** 353–364.
4. Hori, A. (1991) *Cancer Res.* **51,** 6180–6184.
5. Kim, K. J. (1993) *Nature (London)* **362,** 841–844.
6. O'Reilly, M. S., Holmgren, L., Shing, Y., Chen, C., Rosenthal, R. A., Moses, M., Lane, W. S., Cao, Y., Sage, E. H. & Folkman, J. (1994) *Cell* **79,** 315–328.
7. O'Reilly, M. O., Boehm, T., Shing, Y., Fukai, N., Vasios, G., Lane, W. S., Flynn, E., Birkhead, J. R., Olsen, B. R. & Folkman, J. (1997) *Cell* **88,** 277–285.
8. Clapp, C., Martial, J. A., Guzman, R. C., Rentier-Delrue, F. & Weiner, R. I. (1993) *Endocrinology* **133,** 1292–1299.
9. Gupta, S. K., Hassel, T. & Singh, J. P. (1995) *Proc. Natl. Acad. Sci. USA* **92,** 7799–7803.
10. Dong, Z., Kumar, R., Yang, X. & Fidler, I. (1997) *Cell* **88,** 801–810.
11. O'Reilly, M., Holmgren, L., Chen, C. & Folkman, J. (1996) *Nat. Med.* **2,** 689–692.
12. Cao, Y., Ji, R. W., Davidson, D., Schaller, J., Marti, D., Söhndel, S., McCance, S. G., O'Reilly, M. S., Llinas, M. & Folkman, J. (1996) *J. Biol. Chem.* **271,** 29461–29467.
13. Roth, J. A. & Christiano, R. J. (1997) *J. Natl. Cancer Inst.* **88,** 21–39.
14. Stratford-Perricaudet, L., Makeh, I., Perricaudet, M. & Briand, P. (1992) *J. Clin. Invest.* **90,** 626–630.
15. Trochon, V., Mabilat, C., Bertrand, P., Legrand, Y., Smadja-Joffe, F., Soria, C., Delpech, B. & Lu, H. (1996) *Int. J. Cancer* **66,** 664–668.
16. Mirshahi, M., Soria, J., Lijnen, H. R., Fleury, V., Bertrand, O., Drouet, J. Y., Caen, J. & Soria, C. (1997) *Fibrinolysis Proteolysis* **11,** 155–163.
17. Pepper, M. S., Montesano, R., Vassalli, J. D. & Orli, L. (1991) *J. Cell. Physiol.* **146,** 170–179.
18. Mirshahi, M., Soria, J. C. S., Faivre, R., Lu, H., Courtney, M., Roitsch, C., Tripier, D. & Caen, J. P. (1989) *Blood* **74,** 1025–1030.
19. Skladanowski, A. & Larsen, A. K. (1997) *Cancer Res.* **57,** 818–823.
20. Lee Sim, B. K., O'Reilly, M. S., Liang, H., Fortier, A. H., He, W., Madsen, J. W., Lapcevich, R. & Nacy, C. A. (1997) *Cancer Res.* **57,** 1329–1334.
21. Hayes, M. L. & Castellino, F. J. (1979) *J. Biol. Chem.* **254,** 8772–8776.
22. Weidner, N., Semple, J. P. & Welch, W. R. (1991) *N. Engl. J. Med.* **324,** 1–8.
23. Yeh, P. & Perricaudet, M. (1997) *FASEB J.* **11,** 615–623.
24. Davis, F. M., Tsao, T. Y., Fowler, S. K. & Rao, P. N. (1983) *Proc. Natl. Acad. Sci. USA* **80,** 2926–2930.
25. King, R. W., Jackson, P. K. & Kirschner, M. W. (1994) *Cell* **18,** 563–571.
26. Plate, K. H., Breier, G., Weich, H. A. & Risau, W. (1992) *Nature (London)* **359,** 845–848.
27. Hamada, J., Cavanaugh, P. G., Lotan, O. & Nicolson, G. L. (1992) *Br. J. Cancer* **66,** 349–354.
28. Graeber, G. G. (1996) *Nature (London)* **379,** 88–91.